



1 **Enhancement of the North Atlantic CO₂ sink by Arctic Waters**

2 Jon Olafsson¹, Solveig R. Olafsdottir², Taro Takahashi^{3,5}, Magnus Danielsen² and Thorarinn
3 S. Arnarson^{4,5}

4
5 ¹Institute of Earth Sciences, Sturlugata 7 Askja, University of Iceland, IS 101 Reykjavik,
6 Iceland. jo@hi.is

7 ²Marine and Freshwater Research Institute, Fornubúðir 5, IS 220 Hafnafjörður, Iceland

8 ³Lamont-Doherty Earth Observatory of Columbia University, Palisades, NY 10964, U.S.A.

9 ⁴National Energy Authority, Grensásvegur 9, IS 108 Reykjavík, Iceland
10 ⁵Deceased

11

12 **Abstract**

13 The North Atlantic north of 50°N is one of the most intense ocean sink areas for atmospheric
14 CO₂ considering the flux per unit area, 0.27 Pg-C yr⁻¹, equivalent to -2.5 mol C m⁻² yr⁻¹. The
15 Northwest Atlantic Ocean is a region with high anthropogenic carbon inventories. This is on
16 account of processes which sustain CO₂ air-sea fluxes, in particular strong seasonal winds,
17 ocean heat loss, deep convective mixing and CO₂ drawdown by primary production. The
18 region is in the northern limb of the Global Thermohaline Circulation, a path for the long term
19 deep sea sequestration of carbon dioxide. The surface water masses in the North Atlantic are
20 of contrasting origins and character, on the one hand the northward flowing North Atlantic
21 Drift, a Gulf Stream offspring, on the other hand southward moving cold low salinity Polar
22 and Arctic Waters with signatures from Arctic freshwater sources. We have studied by
23 observations, the CO₂ air-sea flux of the relevant water masses in the vicinity of Iceland in all
24 seasons and in different years. Here we show that the highest ocean CO₂ influx is to the
25 Arctic and Polar waters, respectively, -3.8 mol C m⁻² yr⁻¹ and -4.4 mol C m⁻² yr⁻¹. These
26 waters are CO₂ undersaturated in all seasons. The Atlantic Water is a weak or neutral sink,
27 near CO₂ saturation, after poleward drift from subtropical latitudes. These characteristics of
28 the three water masses are confirmed by data from observations covering 30 years. We relate
29 the Polar and Arctic Water persistent undersaturation and CO₂ influx to the excess alkalinity
30 derived from Arctic sources, particularly the Arctic rivers. Carbonate chemistry equilibrium
31 calculations indicate clearly that the excess alkalinity may support a significant portion of the
32 North Atlantic CO₂ sink. The Arctic contribution to the North Atlantic CO₂ sink which we
33 reveal is previously unrecognized. However, we point out that there are gaps and conflicts in
34 the knowledge about the Arctic alkalinity budget and that future trends in the North Atlantic
35 CO₂ sink are connected to developments in the rapidly warming Arctic. The results we



36 present need to be taken into consideration for the question: Will the North Atlantic continue
37 to absorb CO₂ in the future as it has in the past?

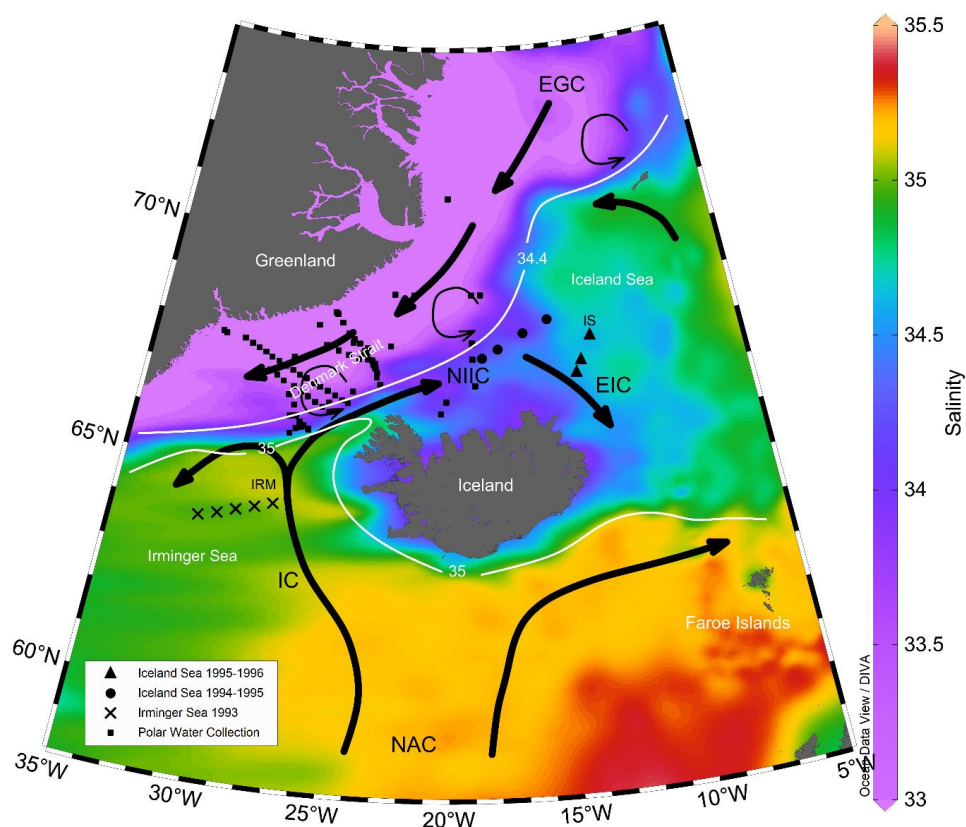
38

39 **1 Introduction**

40 The oceans take up about a quarter of the annual anthropogenic CO₂ emissions (Friedlingstein
41 et al., 2019). The North Atlantic north of 50°N is one of the most intense ocean sink areas for
42 atmospheric CO₂ considering the flux per unit area (Takahashi et al., 2009). The reasons are
43 strong winds and large natural partial pressure differences, $\Delta p\text{CO}_2 = (p\text{CO}_{2\text{sw}} - p\text{CO}_{2\text{a}})$,
44 between the atmosphere and the surface ocean. The $\Delta p\text{CO}_2$ in seawater is a measure of the
45 escaping tendency of CO₂ from seawater to the overlying air. The $\Delta p\text{CO}_2$ is proportional to
46 the concentration of undissociated CO₂ molecules, [CO₂]aq, which constitutes about 1 % of
47 the total CO₂ dissolved in seawater (the remainders being about 90-95 % as [HCO₃⁻] and 4-9
48 % as [CO₃²⁻]). The seawater $p\text{CO}_2$ depends sensitively on temperature and the TCO₂/Alk
49 ratio, the relative concentrations of total CO₂ species dissolved in seawater (TCO₂ = [CO₂]aq
50 + [HCO₃⁻] + [CO₃²⁻]) and the alkalinity, Alk, which reflects the ionic balance in seawater.
51 Large $\Delta p\text{CO}_2$ has been attributed to, a) a cooling effect on the CO₂ solubility in the poleward
52 flowing Atlantic Water, b) an efficient biological drawdown of $p\text{CO}_2$ in nutrient rich subpolar
53 waters and c) high wind speeds over these low $p\text{CO}_2$ waters (Takahashi et al., 2002).
54 Evaluations of $\Delta p\text{CO}_2$ based on observation and models have indicated that the Atlantic north
55 of 50°N and northward into the Arctic takes up as much as 0.27 Pg-C yr⁻¹, equivalent to -2.5
56 mol C m⁻² yr⁻¹ (Takahashi et al., 2009; Schuster et al., 2013; Landschützer et al., 2013; Mikaloff
57 Fletcher et al., 2006). Estimates of long term trends for the North Atlantic CO₂ sink due to
58 changes in either $\Delta p\text{CO}_2$ or wind strength are conflicting, particularly the Atlantic Water
59 dominated regions (Schuster et al., 2013; Landschützer et al., 2013; Wanninkhof et al., 2013).
60 The drivers of seasonal flux variations are inadequately understood (Schuster et al., 2013) and
61 a mechanistic understanding of high latitude CO₂ sinks is considered incomplete (McKinley
62 et al., 2017). It is common to many large scale flux evaluations, modelled or from
63 observations, that they are based on regions defined by geographical borders, latitude and
64 longitude, e.g. between 49°N and 76°N for the high latitude Sub Polar North Atlantic
65 (Takahashi et al., 2009; Schuster et al., 2013). The influence of oceanographic property
66 differences within this region on CO₂ fluxes has thus not been apparent, primarily due to
67 Arctic latitude data limitations. The ability of current generation Earth System Models to
68 predict trends in North Atlantic CO₂ has recently been questioned and suggested that their



69 inadequacies may be caused by biased alkalinity in the simulated background biogeochemical
70 state (Lebehot et al., 2019).



71
72

73 **Figure 1. Mean July to September surface salinity in the vicinity of Iceland.** The $S=35$
74 isohaline marks the boundary between northward flowing Atlantic Water and southward
75 flowing cold Arctic Water and low salinity Polar Water. Stations in Irminger Sea marked X
76 and stations in Iceland Sea marked ● for 1994-1995 and ▲ for 1995-1996 observations.
77 Collection of Polar Water stations 1983-2012 marked ■. IRM and IS mark the location of time
78 series stations. NAC: North Atlantic Current, IC: Irminger Current, NIIC: North Iceland
79 Irminger Current, EIC: East Icelandic Current, EGC: East Greenland Current. Map based
80 on the NISE dataset (Nilsen et al., 2008) and drawn using the Ocean Data View program
81 (Schlitzer, 2018).

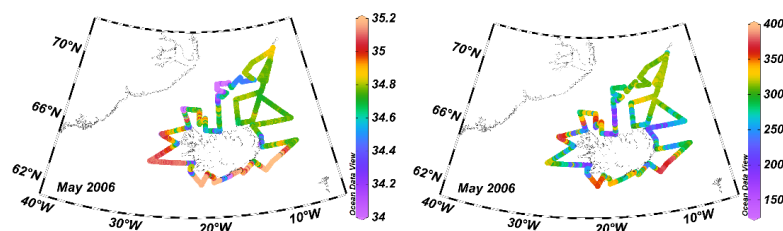
82
83



84 The high latitude North Atlantic Ocean in the vicinity of Iceland, is a region of contrasting
85 surface properties (Fig. 1). The northward flowing North Atlantic Current carries relatively
86 warm and saline Atlantic Water, derived from the Gulf Stream, as far as the Nordic Seas and
87 the Arctic Ocean north of Svalbard. The Irminger Current branch carries Atlantic Water to
88 south and west Iceland and a small branch, the North Icelandic Irminger Current that
89 transports 1 Sv (1 Sv= $10^6 \text{ m}^3 \text{ s}^{-1}$), reaches the Iceland Sea (Stefánsson, 1962;Våge et al.,
90 2011). The rapid East Greenland Current (EGC) (Håvik et al., 2017) flows southward from
91 the Arctic to the North Atlantic, carrying Polar Water cold and with low salinity, $S < 34.4$, due
92 to ice melt and the large freshwater input to the Arctic from rivers that contribute about 11%
93 of the global riverine discharge (Sutherland et al., 2009;McClelland et al., 2012). In between
94 these extremes there are large areas of the Greenland and Iceland Seas that contain
95 predominantly the intermediate, Arctic Water which is a product of heat loss and freshwater
96 export from the EGC (Fig. 1) (Våge et al., 2015). The north- and southward flowing currents
97 are separated by the Arctic Front outlined in Figure 1 by the salinity=35 contour generally
98 oriented SW-NE. Deep water formation in the high latitude North Atlantic produces cold
99 dense waters which, together with a similar product in the Labrador Sea, are source waters for
100 the Global Thermohaline Circulation linking the regional air-sea CO_2 flux to a route for the
101 long term deep ocean sequestration of anthropogenic CO_2 (Broecker, 1991). The region of our
102 study affects large scale ocean-atmosphere CO_2 exchange processes in the North Atlantic.
103 Here we evaluate regional, seasonal and interannual air-sea carbon dioxide fluxes for the main
104 surface waters characteristic of this region (Fig. 1). We base this work on extensive
105 observations which cover regional water masses, all seasons and include different states of the
106 North Atlantic Oscillation, NAO (Flatau et al., 2003). We employ two different observation
107 approaches for flux estimates. Firstly, repeat station hydrography with emphasis on the
108 seasonal flux patterns in Atlantic Water and in Arctic Water (Fig. 1). Secondly, underway
109 ship records of surface $p\text{CO}_2$ where the emphasis was on the different surface water masses
110 (Fig. 2).

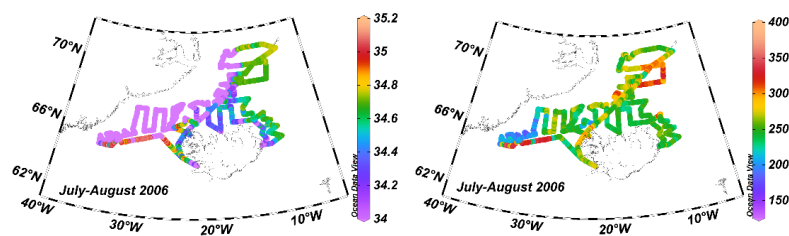
111

112

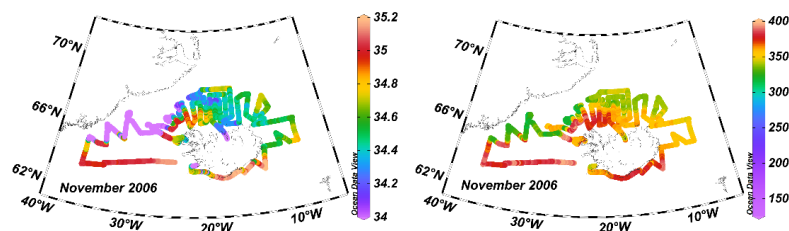




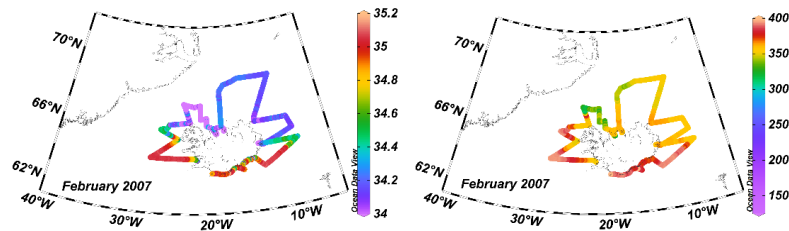
113



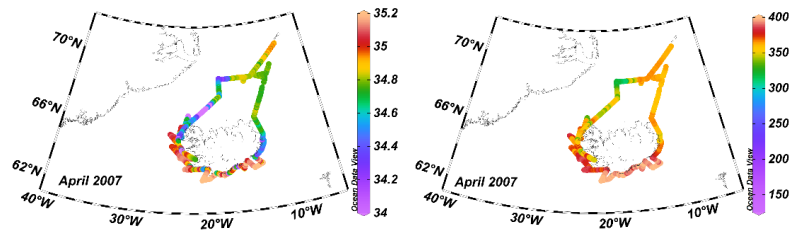
114



115



116



117

118

119

120

121

122

123

124

125

126

Figure 2. Cruise tracks where surface layer salinity and $p\text{CO}_2$ were recorded underway. Left sea surface salinity, right $p\text{CO}_2\text{sw}(\mu\text{atm})$ along the cruise tracks. Maps drawn using the Ocean Data View program (Schlitzer, 2018).

We describe long term carbon chemistry characteristics of water masses in mid winter when physical forces prevail over biological processes. For the Irminger Sea and Iceland Sea from



127 time series observations (Olafsson et al., 2010) and for the EGC Polar Water from a collection
128 of $p\text{CO}_2$ data assembled in the period 1983 to 2012.

129

130 **2 Methods**

131 **2.1 Data acquisition**

132 Seasonal carbon chemistry variations in the relatively warm and saline ($S > 35$) Atlantic Water
133 were studied 1993-1994 on 15 cruises from February 1993 to January 1994 to 5 stations on a
134 167 km long transect over the core of the Irminger Current and into the northern Irminger Sea
135 (Fig. 1 and Tables S1 and S2). In order to close the full annual cycle, to 23 February 1994 we
136 use data from the previous year and date. In 1994-1996 the study centered on the colder and
137 less saline Arctic Water of the Iceland Sea and was conducted on 22 cruises with sampling
138 dates from 11 Feb 1994 to 12 Feb 1996, two years. In 1994 on 4 stations on a 168 km long
139 transect into the Iceland Sea Gyre and in 1995 on 3 stations across the East Icelandic Current
140 (Fig. 1 and Tables S1 and S3 in the supplement). On each cruise the station work was
141 completed in 1-2 days. For both regions, the timing of cruises was with the period of the
142 phytoplankton spring bloom in mind (Takahashi et al., 1993b). The work was conducted on
143 vessels operated by the Marine Research Institute (MRI) in Reykjavik, Iceland, R/V Bjarni
144 Seamundsson and R/V Arni Fridriksson. Three times in 1994 a fishing vessel M/V Solrun,
145 was hired. In August 1994 the stations were completed on the Norwegian vessel R/V Johann
146 Hjort.

147 Discrete surface layer, 1m, 5m and 10m, $p\text{CO}_2$ samples were collected into 500 ml volumetric
148 flasks from water bottles on a Rosette and Sea Bird 911 CTD instruments. The samples were
149 preserved with mercuric chloride and analysed ashore by equilibration at 4°C with a gas of
150 known CO_2 concentration followed by gas chromatography with a flame ionization detector.
151 The instrument was calibrated with N_2 reference gas and 3 standards, 197.85 ppm, 362.6 ppm
152 and 811.08 ppm, calibrated against standards certified by NOAA-CMDL at Boulder, CO,
153 USA. So were also calibrated the standards used for the underway measurements (Chipman et
154 al., 1993). Quality assurance and sample storage experiments indicated an overall precision of
155 the $p\text{CO}_2$ determinations better than $\pm 2 \mu\text{atm}$ (Olafsson et al., 2010).

156 The underway $p\text{CO}_2$ determinations in 2006-2007 covered areas of the East Greenland
157 Current in and northwards from the Denmark Strait, in addition to Atlantic and Arctic Waters.
158 The 6 cruises (Table S4) covered all seasons and all three water masses but with variable areal
159 extensions (Fig. 2 and S1). Seawater was pumped continuously from an intake at 5 m depth
160 at 10 L min^{-1} into a shower-head equilibrator with a total volume of 30 L and a headspace of



161 15 L. Temperature at the inlet and salinity were measured with an SeaBird Model SBE-21
162 thermosalinograph (Sea-Bird Electronics, Seattle, WA, USA). Underway $p\text{CO}_2$ determinations
163 were carried out with a system similar to the one described by Bates and coworkers (Bates et
164 al., 1998). The mole fraction of CO_2 ($V \text{ CO}_2$) in the headspace was determined with a Li-Cor
165 infrared analyzer Model 6251 (Li-Cor Biosciences, Lincoln, NB, USA). The instrument was
166 calibrated against four standards of CO_2 in air certified by NOAA-CMDL at Boulder, CO,
167 USA. and a N_2 reference gas. The standards had CO_2 dry air mole fractions of 122.19,
168 253.76, 358.41 and 476.81 ppm. The $p\text{CO}_2$ sw determinations were corrected to in-situ
169 seawater temperatures using the equation (Takahashi et al., 1993b):

$$170 \quad p\text{CO}_2 \text{ sw}(\text{in situ}) = p\text{CO}_2 \text{ sw}(\text{eq}) e^{0.0423(T_{\text{in situ}} - T_{\text{eq}})} \quad (\text{eq.1})$$

171 The sample processing and quality control measures have been described in detail (Olafsson
172 et al., 2010).

173 Polar Water collection. Discrete samples for carbon chemistry studies were taken on stations
174 ($N=97$) in the East Greenland Current when opportunities permitted on cruises in the period
175 1983 to 2012. The data provide $p\text{CO}_2$ for calculation of Delta $p\text{CO}_2$ in Fig. 4.

176

177 **2.2 CO_2 air-sea flux calculations**

178 In this study, the $p\text{CO}_2$ in seawater samples has been measured by gas-seawater equilibration
179 methods (Olafsson et al., 2010). The bulk flux of the carbon dioxide across the air-sea
180 interface is often estimated from its relationship with wind speed and sea-air partial pressure
181 difference, $\Delta p\text{CO}_2$. We determine the flux (F) from $\Delta p\text{CO}_2$ and use Eq. 1 and Eq. 2 for
182 estimating the bulk air-sea fluxes of CO_2 (Takahashi et al., 2009)

$$183 \quad F = k \cdot \alpha \cdot \Delta p\text{CO}_2 \quad (\text{Eq 1})$$

$$184 \quad F = 0.251 U^2 (S_c/660)^{-0.5} \alpha (p\text{CO}_{2 \text{ w}} - p\text{CO}_{2 \text{ a}}) \quad (\text{Eq 2})$$

185 There $k=0.251 U^2 (S_c/660)^{-0.5}$ is the gas transfer velocity or kinetic component of the
186 expression (Wanninkhof, 2014), α is the solubility of CO_2 gas in sea water (Weiss, 1974) and
187 $\Delta p\text{CO}_2 = (p\text{CO}_{2 \text{ sw}} - p\text{CO}_{2 \text{ a}})$, is the partial pressure difference or thermodynamic component of
188 the expression (Takahashi et al., 2009). For the wind speed, U , we use the CCMP-2
189 reanalysis wind product (Wanninkhof, 2014; Atlas et al., 2011; Wanninkhof and Triñanes,
190 2017).

191 The atmospheric partial pressure values, $p\text{CO}_{2 \text{ a}}$, used in the $\Delta p\text{CO}_2$ calculations are weekly
192 averages from the GLOBALVIEW- CO_2 database for the CO_2 -ICE location which is at
193 Vestmannaeyjar islands, off south Iceland (GLOBALVIEW- CO_2 , 2013). Mauna Loa values



194 were used for periods where CO₂-ICE data was missing (Tans and Keeling, 2019). The dry
195 air V CO₂ mole fraction values were converted to μatm using $p\text{CO}_2 (\mu\text{atm}) = V \text{CO}_2 (P_a - P_w)$
196 where P_a is the barometric pressure and P_w is the equilibrium water vapour pressure.

197

198 For the Irminger Sea seasonal study we use 30 day running means of the squared daily wind
199 speed for the region 63.5°N to 64.5°N and 27°W to 32°W and for the Iceland Sea seasonal
200 study a similar wind product for the region 66.5°N to 68.5°N and 12°W to 19°W. Fluxes
201 were calculated for the periods between cruises from interpolated $p\text{CO}_2$ data and period mean
202 30 day squared wind running means data. There are thus 14 flux periods covering a year for
203 the Irminger sea and 21 flux periods covering two years in the Iceland Sea (Tables S1 and S2
204 in the supplement). The annual fluxes were found by summation of the period fluxes (Table
205 1).

206 For the underway cruises 2006 to 2007 we used CCMP-2 daily wind fields at 1x1 degree for
207 the region 62°N to 72°N and 5°W to 40°W. This region was further divided into 4 sub-
208 regions by latitude 64.9°N and longitude 20°W. Daily 30 day running means of the squared
209 wind speed from two locations in each sub-region were extracted and their means used for
210 flux calculations when the vessel sailed in the area. Fluxes were calculated for all $p\text{CO}_2$ data
211 from the 6 cruises, in total 42938 measurements.

212 The flux data from each of the 6 cruises were categorized into the three sea water types using
213 the following criteria:

- 214 1) Atlantic Water $S > 35$, Arctic Water $S: 34.4-34.9$, Polar Water < 34.4 .
- 215 2) Seasonal salinity and temperature variations were taken into account.
- 216 3) Waters with runoff influences from Iceland were excluded using salinity and ship
217 position data.

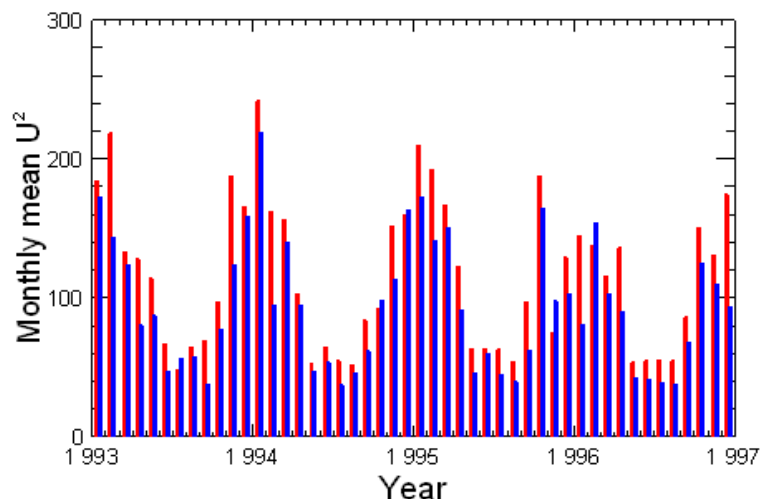
218 Thus a total of 33352 measurements were used, or 78% of the flux data points. The CO₂
219 fluxes in the realm of each water mass were assessed for the duration of each cruise by
220 numerical integration. Fluxes in the 5 periods between cruises were assessed by interpolation
221 of temperature, salinity and $p\text{CO}_2$ for each water mass and by using period regional 30 day
222 running means of squared wind speed data. The annual flux for each water mass was assessed
223 by summation.

224

225 3 Results

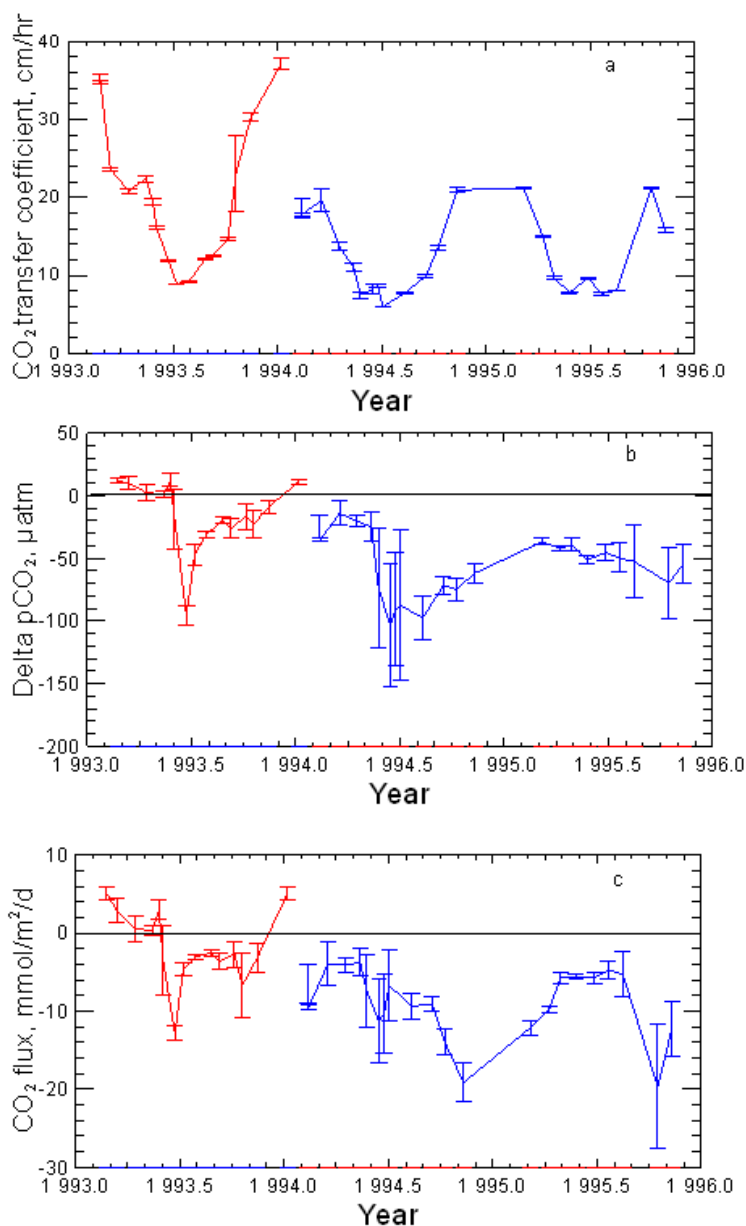


226 Mean monthly reanalysis of winds reveal seasonal variations with strong winds in winter
227 when they may be stronger over the Irminger Sea than the Iceland Sea as in 1993-1994 and in
228 1994-1995 (Fig. 3).



229
230 **Figure 3. Monthly means of squared CCMP-2 daily winds, U m/s. Irminger Sea region (red)**
231 **and the Iceland Sea region (blue).**
232

233 The cyclone tracks in the atmosphere, particularly of the Icelandic Low, influence the regional
234 conditions which may change abruptly as in the 1994-1996 period or become anomalous as in
235 1995 when cold northeasterly winds persisted north of Iceland under positive NAO conditions
236 (Ólafsson, 1999; Flatau et al., 2003). Both the Irminger Sea and the Iceland Sea seasonal
237 studies reveal the strongest CO_2 undersaturation, with negative $\Delta p\text{CO}_2$ of about $100 \mu\text{atm}$ in
238 May at the time of the phytoplankton spring bloom (Fig. 4). The undersaturation diminishes
239 through the summer and autumn followed by a gradual return to winter conditions (Fig. 4b)
240 (Takahashi et al., 1985; Takahashi et al., 1993a).
241



242

243

244

245

246

247

248

249

250

251

252

253

254

Figure 4. Seasonal variations in the Atlantic Water of the Irminger Sea (red) and in the Arctic Water of the Iceland Sea (blue). The gas transfer velocity (a) reflects the seasonal wind strength and the error bars its variations during intervals between cruises. Delta pCO₂ (b) records the tendency for CO₂ to be transferred to the atmosphere (positive) or from the atmosphere to the ocean (negative). The CO₂ flux rate (c) reveals that the Arctic Water is a CO₂ sink in all seasons whereas the Atlantic Water is a source in winter and a weak sink at other times of the year. The error bars indicate ± 1 standard deviation from the mean and reflect the variations between the stations observed each cruise.



255

256 The CO₂ influx in the spring is, however, relatively small as the wind gas transfer coefficient
257 is then moderate (Fig.4a). In the autumn the winds strengthen with heat loss and vertical
258 mixing while CO₂ undersaturation still persists. In mid winter, February-March, vertical
259 mixing brings richer CO₂ water to the surface of the Irminger Sea leading to supersaturation
260 (Ólafsson, 2003), the flux reverses and the region becomes a weak source for atmospheric
261 CO₂ (Fig. 4c).

262

263 **Table 1 Annual sea–air CO₂ fluxes (mol C m⁻² y⁻¹) in the three water masses.**

Water masses and evaluation methods	CO ₂ flux mol C m ⁻² y ⁻¹
Atlantic water, repeat stations 1993	-0.69±0.16
Atlantic water, Underway Measurements, 2006-2007	0.07 ± 0.15
Arctic water, repeat stations 1994	-3.97±0.48
Arctic water, repeat stations 1995	-3.60±0.31
Arctic water, Underway Measurements, 2006-2007	-2.84 ± 0.19
Polar water, Underway Measurements, 2006-2007	-4.44 ± 0.34

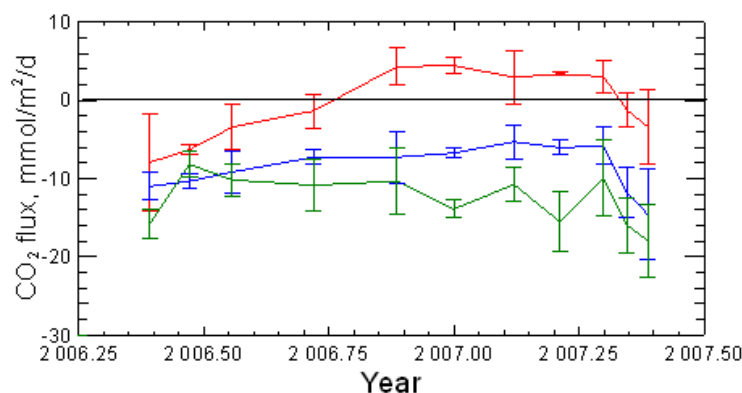
264

265 The integrated annual CO₂ flux shows that the Atlantic Water in the Irminger Sea was a weak
266 sink, -0.69±0.16 mol C m⁻² y⁻¹, in 1993 (Table 1). The more extensive underway area
267 coverage of the Atlantic Water in 2006-2007, confirmed in essence the seasonal pattern and
268 indicated that the Atlantic Water was a neutral sink, 0.07 ± 0.15 mol C m⁻² y⁻¹ for this year
269 (Table 1).

270 The years of the Iceland Sea observations, 1994-1996, coincided with a large transition in the
271 North Atlantic Oscillation (NAO) from a positive state 1994/1995 to a negative state in
272 1995/1996 and large scale shifts in ocean fronts (Flatau et al., 2003). Vertical density
273 distribution in the Iceland Sea indicated an enhanced convective activity in 1995 (Våge et al.,
274 2015). Cold northeasterly winds were persistent in the spring of 1995 resulting in record low
275 temperature anomalies for the north Iceland shelf (Ólafsson, 1999). In 1995 the spring bloom
276 associated undersaturation, ΔpCO₂, was only half of that in 1994, possibly due to a weaker
277 stratification (Fig. 4b). As in the Irminger Sea the spring bloom associated CO₂ influx is
278 small. The largest CO₂ influx was in the fall and early winters of 1995 and 1996 as
279 temperature dropped, winds gathered strength and vertical mixing was enhanced. This

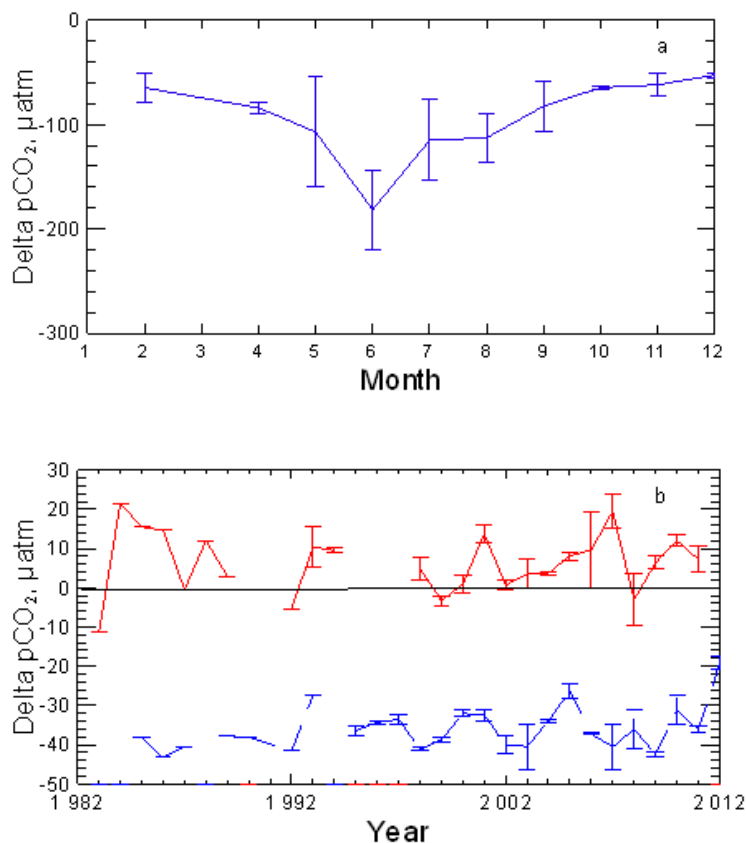


280 compensated for the small spring bloom in 1995 and the annual bulk fluxes 1994 and 1995 are
281 similar and high despite very different physical conditions (Table 1). The UW p CO $_2$ surveys
282 had less temporal resolution but confirmed all year undersaturation of the Arctic Water.
283 However, the integrated annual influx, $-2.84 \text{ mol C m}^{-2} \text{ y}^{-1}$, was significantly less than
284 evaluated with repeat station data (Table 1, Fig.5). This may reflect the large underway area
285 coverage compared with the repeated fixed stations.



286
287 **Figure 5. Seasonal air-sea CO $_2$ flux variations from UW p CO $_2$ observations.** Atlantic Water
288 (red) is a weak sink in summer and neutral over the year, $n=7068$. Both Arctic Water (blue)
289 $n=16874$, and Polar Water (green) $n=9410$, are strong sinks throughout the year. The error
290 bars indicate ± 1 standard deviation from the mean.

291
292 Ice cover in the East Greenland Current is variable and the ice edge at the seasonal minimum
293 has moved northward and from the Denmark Strait with decreasing Arctic sea ice (Serreze
294 and Meier, 2019). The Polar Water salinity ranges from 34.4 to less than 30 in summer. The
295 lowest salinity water freezes leading to salinity around 34 in winter. We covered the Polar
296 Water in all six UW p CO $_2$ surveys 2006-2007 (Supplement Fig. S1) and undersaturation
297 characterised this water mass in all cruises. The integrated annual influx, $-4.44 \text{ mol C m}^{-2} \text{ y}^{-1}$
298 (Table 1, Fig.5), shows the Polar Water to be the strongest CO $_2$ sink, 80 % above the
299 estimated mean for the Atlantic north of 50°N, $-2.5 \text{ mol C m}^{-2} \text{ y}^{-1}$ (Takahashi et al., 2009).
300 We evaluate the long term p CO $_2$ characteristics of the three water masses from other data
301 assembled over about 30 years. A composite picture of seasonal Δp CO $_2$ variations in Polar
302 Water in and north of the Denmark Strait (Fig.1) confirms all year undersaturation, deep from
303 biological drawdown in summer, and in mid winter when salinity raises to ~ 34 , the Δp CO $_2$
304 levels at about $-50 \mu\text{atm}$ (Fig. 6a). Long term winter Δp CO $_2$ in the Irminger Sea and Iceland
305 Sea (Figs. 1 and 6 b) show the Atlantic Water to be near saturation whereas the Arctic
306 Water is undersaturated to about $-35 \mu\text{atm}$.



307
308

309

310 **Figure 6. Water mass decadal surface water $p\text{CO}_2$ characteristics.** a) A composite picture of
311 $\Delta p\text{CO}_2$ from 97 stations with Polar Water $p\text{CO}_2$ observations ($n=280$) 1983 to 2012
312 shows undersaturation at all times of the year. The error bars indicate ± 1 standard deviation
313 from the monthly means. b) Atlantic Water at the Irminger Sea time series station (red) is
314 generally a weak CO_2 source in winter (24 winters, 52 samples), January-March, whereas
315 winter (25 winters, 61 samples) CO_2 undersaturation persists in the Iceland Sea time series
316 site (blue). The error bars indicate ± 1 standard deviation from the station means.

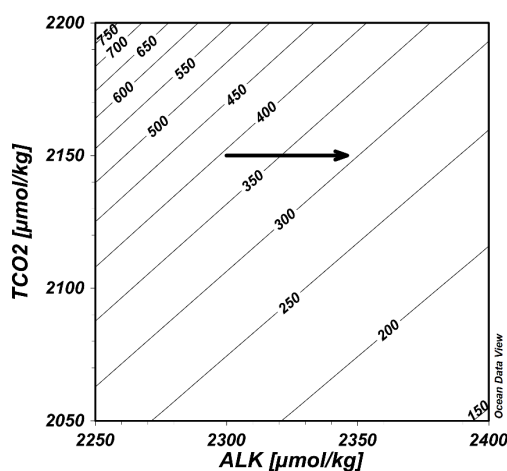
317
318

319 4 Discussion

320 The carbonate chemistry of Polar Water differs from that of open ocean waters, e.g. Atlantic
321 Water, in having an increasingly higher alkalinity/salinity and alkalinity/ TCO_2 ratios as the
322 salinity decreases from about $S=34.4$. The excess alkalinity has been attributed to the high
323 riverine input from continents to the Arctic (Anderson et al., 2004; Lee et al., 2006). The flow-
324 weighted average alkalinity of 6 major Arctic rivers, discharging $2.245 \times 10^3 \text{ km}^3 \text{ yr}^{-1}$, is 1048
325 $\mu\text{mol kg}^{-1}$ (Cooper et al., 2008). Linear alkalinity-salinity relationships observed in the Arctic
326 Ocean and the Nordic Seas and their extrapolated intercepts to $S=0$, have indicated freshwater



327 sources with alkalinity $1412 \mu\text{mol kg}^{-1}$ (Anderson et al., 2004) and $1752 \mu\text{mol kg}^{-1}$ (Nondal
328 et al., 2009). Climatological data from the West- Greenland, Iceland and Norwegian Seas
329 show a high $S=0$ intercept of $1796 \mu\text{mol kg}^{-1}$ but a lower one for the High Arctic north of
330 80°N , $1341 \mu\text{mol kg}^{-1}$ (Takahashi et al., 2014). The intercepts may be interpreted as the mean
331 alkalinity of fresh waters added to the Arctic by rivers and melting ice and snow. However,
332 the intercepts indicate considerable variability, they are higher than the average alkalinity of
333 Arctic rivers and the intercepts are high in upstream regions of the East Greenland Current.
334 The excess alkalinity would lower the $p\text{CO}_2$ in seawater (and increase the pH), and thus give
335 it an increased capacity to take up CO_2 from the air (Fig. 7). The thermodynamic driving
336 force for seawater CO_2 uptake, $(p\text{CO}_{2\text{sw}} - p\text{CO}_{2\text{a}})$, is enhanced.
337



338

339 **Figure 7. Thermodynamic relations of alkalinity, total inorganic carbon and the**
340 **equilibrium $p\text{CO}_2$ in seawater (μatm).** Calculated for $S=35$ and temperature 5°C , typical for
341 Atlantic Water which reaches the Nordic Seas. The slope of the $350 \mu\text{atm}$ $p\text{CO}_2$ contour has a
342 value of 0.85 and describes the relative extent of alkalinity and TCO_2 additions (ΔTCO_2
343 $/\Delta\text{Alk}$) to maintain unchanged $p\text{CO}_2$. The arrow illustrates that an $46 \mu\text{mol kg}^{-1}$ alkalinity
344 excess decreases $p\text{CO}_2$ by $88 \mu\text{atm}$, causes undersaturation. Figure drawn using the Ocean
345 Data View program (Schlitzer, 2018).

346 How large is the effect of Arctic alkalinity inputs on the CO_2 uptake by the Nordic Seas and
347 the North Atlantic? We consider two ways to make this estimate. Firstly, from the river
348 runoff into the Arctic which is estimated to be about $4.2 \times 10^3 \text{ km}^3 \text{ yr}^{-1}$, or $0.133 \times 10^6 \text{ m}^3 \text{ s}^{-1}$



349 (0.133 Sv). This is about 11% of the global freshwater input to the oceans (Carmack et al.,
350 2016). Taking the average alkalinity $1048 \mu\text{mol kg}^{-1}$, the amount of alkalinity added by rivers
351 to the Arctic and transported to the North Atlantic via the Canadian Arctic Arcipelago and via
352 the Fram Strait and further south with the Labrador and East Greenland Currents, would be 4.4
353 $\times 10^{12} \text{ mol yr}^{-1}$ (Supplement). The $p\text{CO}_2$ of seawater would be reduced by an addition of this
354 much excess alkalinity. Let us suppose that the $p\text{CO}_2$ in seawater was restored to the original
355 value by absorbing CO_2 from the atmosphere. The carbonate equilibrium relations in
356 seawater give that $p\text{CO}_2$ is unchanged if $\Delta\text{TCO}_2 / \Delta\text{Alk} = 0.85$ (Fig. 6). This ratio is nearly
357 constant in the temperature and salinity range of the subarctic North Atlantic surface waters.
358 Therefore, the Arctic river alkalinity would contribute to an uptake of CO_2 from the
359 atmosphere of $3.73 \times 10^{12} \text{ mol CO}_2 \text{ yr}^{-1}$ or $0.045 \text{ Pg-C yr}^{-1}$ (Supplement).

360 Second estimate. The volume transport of Polar Water, density $<1027.8 \text{ kg m}^{-3}$, by the EGC
361 has recently been estimated as 3.9 Sv (Våge et al., 2013). Taking $S=33.0$ for the mean Polar
362 Water salinity and using Equations 6 and 7 in Nondal et al (2009), the mean Polar Water
363 alkalinity is $2256 \mu\text{mol kg}^{-1}$ which is $46 \mu\text{mol kg}^{-1}$ more alkalinity than the Atlantic Water
364 calculated at the same salinity (Nondal et al., 2009). This much excess alkalinity would lower
365 the $p\text{CO}_2$ of Atlantic Water by $88 \mu\text{atm}$ and increase the pH by 0.10 (Fig. 7). Thus, the
366 excess alkalinity advected to the North Atlantic by the EGC is $5.7 \times 10^{12} \text{ mol yr}^{-1}$. Using
367 again 0.85 for the $\Delta\text{TCO}_2 / \Delta\text{Alk}$ changes at a constant $p\text{CO}_2$, we obtain that the contribution of
368 the excess EGC alkalinity to the uptake of CO_2 from the atmosphere would be $34.8 \times 10^{12} \text{ mol}$
369 $\text{CO}_2 \text{ yr}^{-1}$, or $0.058 \text{ Pg-C yr}^{-1}$. The two estimates correspond to 17% and 21 %, respectively,
370 of the net CO_2 uptake of $0.27 \text{ Pg-C yr}^{-1}$ for the subarctic oceans north of 50°N (Takahashi et
371 al., 2009). We did not include in the second estimate any alkalinity contribution with the
372 considerable Canadian Arctic Arcipelago Polar Water freshwater transport (Haine et al.,
373 2015). The effect of excess alkalinity on the oceanic CO_2 uptake flux may therefore be
374 substantially greater than our calculated estimates. We note that the winter undersaturation
375 levels, of $-50 \mu\text{atm}$ and $-35 \mu\text{atm}$ observed in the Polar and Arctic Waters, respectively (Fig.
376 5), translate to excess alkalinity of $19 \mu\text{mol kg}^{-1}$ and $21 \mu\text{mol kg}^{-1}$ for further CO_2 influx
377 downstream.

378 The difference between the average measured Arctic river alkalinity and the regression based
379 estimates of alkalinity sources suggests that other origins and processes than the rivers
380 contribute to the Polar Water alkalinity exported with currents from the Arctic to the Atlantic
381 Ocean. Photic layer primary production in the absence of calcification may lower the



382 TCO₂/Alk ratio and seawater *p*CO₂ in marginal seas (Bates, 2006), while acidification is
383 increasing in other regions (Anderson et al., 2017; Qi et al., 2017). Furthermore, the sea-ice
384 seasonal formation and melting may affect the TCO₂/Alk ratio (Grimm et al., 2016; Rysgaard
385 et al., 2007). The Arctic is complex and complex climate warming related changes are
386 observed in the western Arctic Ocean (Ouyang et al., 2020) and expected in marine
387 freshwater systems of the warming Arctic (Carmack et al., 2016). River water alkalinity
388 increases with an addition of cations derived from the chemical weathering of silicate and
389 carbonate rocks (Bernier and Bernier, 1987). Accordingly, an increase in Arctic weathering
390 rates, in response to warmer climate and increasing atmospheric CO₂, could increase the river
391 water alkalinity transported into the oceans. Such an increase would lower the *p*CO₂ in
392 seawater and enhance the oceanic uptake of atmospheric CO₂, providing a negative feedback
393 mechanism to the climatic warming resulting from increased atmospheric CO₂.

394

395 **5 Conclusions**

396 The North Atlantic region we describe has ocean waters advected from southern temperate
397 latitudes and others from the north with Arctic signatures. The Gulf Stream derived Atlantic
398 Water which reaches the northern Irminger Sea and the Nordic Seas, has had a long contact
399 time with the atmosphere to loose heat and reach near CO₂ saturation (Takahashi et al.,
400 2002; Olsen et al., 2006). The Atlantic Water seasonal *p*CO₂ variations we observe (Fig. 2c),
401 are primarily driven by regional thermal and biological cycles (Takahashi et al., 2002). The
402 southward flowing Arctic and Polar Waters are on the contrary strong and persistent all year
403 CO₂ sinks despite various regional changes upstream in the Arctic Ocean. Downstream from
404 the Polar Water and Arctic Water outflows is the subpolar North Atlantic with high water
405 column inventories of anthropogenic carbon (Khatriwala et al., 2013; Gruber et al., 2019). The
406 high anthropogenic CO₂ regions have been attributed, as mentioned above, to the combined
407 effects of the solubility and biology gas exchange pumps on the CO₂ fluxes (Takahashi et al.,
408 2002). We point here to the Polar Water and Arctic Water CO₂ influx and excess alkalinity as
409 an additional unrecognized source contributing to the North Atlantic CO₂ sink. Climate
410 induced changes in Arctic biogeochemistry and alkalinity budget are likely to affect the
411 sensitivity and future strength of the North Atlantic CO₂ sink downstream.

412

413 **Acknowledgements**

414 The NMR Nordic Environmental Research Programme: Carbon Cycle and Convection in the
415 Nordic Seas, supported the Marine Research Institute (MRI), Reykjavik, repeat station study



416 in 1993-1995. The MRI work in 2006-2008 was supported by the European Union 6th
417 Framework Program CARBOOCEAN, EU Contract: 511176. Taro Takahashi was supported
418 to work on the manuscript with a grant from the the US National Oceanographic and
419 Atmospheric Administration. The CCMP-2 wind product was generously provided by Remote
420 Sensing Systems (www.remss.com/measurements/CCMP) by Dr. Joaquin Triñanes of
421 CIMAS/AOML, Miami. We gratefully acknowledge the long term technical support from
422 John Goddard and Tim Newberger, Lamont-Doherty Earth Observatory. We are grateful for
423 the invaluable cooperation we have had with the crews of all vessels operated in this study
424 and to Norwegian colleagues for providing time for station work in August 1994.

425

426

427 *Author Contributions.* J.O., T.T. and S.R.O. wrote the manuscript. J.O., Th.S.A., S.R.O. and
428 M.D. conducted the fieldwork. J.O., T.T. S.R.O. and Th.S.A., conceived this study.

429

430 *AdCompeting interests.* The authors declare no competing financial interests.

431

432

433

434 **References**

435

436 Anderson, L. G., Jutterström, S., Kaltin, S., and Jones, E. P.: Variability in river runoff
437 distribution in the Eurasian Basin of the Arctic Ocean, *Journal of Geophysical Research*, 109,
438 doi:10.1029/2003JC001733, 2004.

439 Anderson, L. G., Ek, J., Ericson, Y., Humborg, C., Semiletov, I., Sundbom, M., and Ulfsbo,
440 A.: Export of calcium carbonate corrosive waters from the East Siberian Sea, *Biogeosciences*,
441 14, 1811-1823, 10.5194/bg-14-1811-2017, 2017.

442 Atlas, R., Hoffman, R. N., Ardizzone, J., Leidner, S. M., Jusem, J. C., Smith, D. K., and
443 Gombos, D.: A cross-calibrated multiplatform ocean surface wind velocity product for
444 meteorological and oceanographic applications, *Bull. Amer. Meteor. Soc.*, 92, 157-174,
445 10.1109/IGARSS.2008.4778804, 2011.

446 Bates, N. R., Takahashi, T., Chipman, D. W., and Knap, A. H.: Variability of pCO₂ on diel to
447 seasonal timescales in the Sargasso Sea near Bermuda, *Journal of Geophysical Research:*
448 *Oceans*, 103, 15567-15585, 10.1029/98jc00247, 1998.

449 Bates, N. R.: Air-sea CO₂ fluxes and the continental shelf pump of carbon in the Chukchi Sea
450 adjacent to the Arctic Ocean, *Journal of Geophysical Research: Oceans*, 111,
451 10.1029/2005jc003083, 2006.

452 Berner, E. K., and Berner, R. A.: *The Global Water Cycle, Geochemistry and Environment*,
453 Prentice-Hall, Englewood Cliffs, NJ, 1987.

454 Broecker, W. S.: The Great Ocean Conveyor, *Oceanography*, 4, 79-89, 1991.

455 Carmack, E. C., Yamamoto-Kawai, M., Haine, T. W. N., Bacon, S., Bluhm, B. A., Lique, C.,
456 Melling, H., Polyakov, I. V., Straneo, F., Timmermans, M.-L., and Williams, W. J.:

457 Freshwater and its role in the Arctic Marine System: Sources, disposition, storage, export, and



458 physical and biogeochemical consequences in the Arctic and global oceans, *J. Geophys. Res.*
459 *Biogeosci.*, 121, 675–717, doi:10.1002/2015JG003140, 2016.

460 Chipman, D., Marra, J., and Takahashi, T.: Primary production at 47°N and 20°W in the
461 North Atlantic Ocean: a comparison between the ¹⁴C incubation method and the mixed layer
462 budget, *Deep Sea Research II*, 40, 151-169, 1993.

463 Cooper, L. W., McClelland, J. W., Holmes, R. M., Raymond, P. A., Gibson, J. J., C. K. Guay,
464 and Peterson, B. J.: Flow-weighted values of runoff tracers ($\delta^{18}\text{O}$, DOC, Ba, alkalinity) from
465 the six largest Arctic rivers, *Geophysical Research Letters*, 35, doi:10.1029/2008GL035007,
466 2008.

467 Flatau, M. K., Talley, L., and Niiler, P. P.: The North Atlantic Oscillation, surface current
468 velocities, and SST changes in the subpolar North Atlantic, *Journal of Climate*, 16, 2355-
469 2369, 2003.

470 Friedlingstein, P., Jones, M. W., O'Sullivan, M., Andrew, R. M., Hauck, J., Peters, G. P.,
471 Peters, W., Pongratz, J., Sitch, S., Le Quééré, C., Bakker, D. C. E., Canadell, J. G., Ciais, P.,
472 Jackson, R. B., Anthoni, P., Barbero, L., Bastos, A., Bastrikov, V., Becker, M., Bopp, L.,
473 Buitenhuis, E., Chandra, N., Chevallier, F., Chini, L. P., Currie, K. I., Feely, R. A., Gehlen,
474 M., Gilfillan, D., Gkritzalis, T., Goll, D. S., Gruber, N., Gutekunst, S., Harris, I., Haverd, V.,
475 Houghton, R. A., Hurtt, G., Ilyina, T., Jain, A. K., Joetzjer, E., Kaplan, J. O., Kato, E., Klein
476 Goldewijk, K., Korsbakken, J. I., Landschützer, P., Lauvset, S. K., Lefèvre, N., Lenton, A.,
477 Lienert, S., Lombardozzi, D., Marland, G., McGuire, P. C., Melton, J. R., Metzl, N., Munro,
478 D. R., Nabel, J. E. M. S., Nakaoka, S. I., Neill, C., Omar, A. M., Ono, T., Pregon, A., Pierrot,
479 D., Poulter, B., Rehder, G., Resplandy, L., Robertson, E., Rödenbeck, C., Séférian, R.,
480 Schwinger, J., Smith, N., Tans, P. P., Tian, H., Tilbrook, B., Tubiello, F. N., van der Werf, G.
481 R., Wiltshire, A. J., and Zaehle, S.: Global Carbon Budget 2019, *Earth Syst. Sci. Data*, 11,
482 1783-1838, 10.5194/essd-11-1783-2019, 2019.

483 GLOBALVIEW-CO2: Cooperative Global Atmospheric Data Integration Project. 2013,
484 updated annually. Multi-laboratory compilation of synchronized and gap-filled atmospheric
485 carbon dioxide records for the period 1979-2012 obspack_co2_1_GLOBALVIEW-
486 CO2_2013_v1.0.4_2013-12-23, 2013.

487 Grimm, R., Notz, D., Glud, R. N., Rysgaard, S., and Six, K. D.: Assessment of the sea-ice
488 carbon pump: Insights from a three-dimensional ocean-sea-ice-biogeochemical model
489 (MPIOM/HAMOCC), *Elementa: Science of the Anthropocene* • 4: 000136 • 4, doi:
490 10.12952/journal.elementa.000136
491 elementascience.org, 2016.

492 Gruber, N., Clement, D., Carter, B. R., Feely, R. A., van Heuven, S., Hoppema, M., Ishii, M.,
493 Key, R. M., Kozyr, A., Lauvset, S. K., Lo Monaco, C., Mathis, J. T., Murata, A., Olsen, A.,
494 Perez, F. F., Sabine, C. L., Tanhua, T., and Wanninkhof, R.: The oceanic sink for
495 anthropogenic CO₂ from 1994 to 2007, *Science*, 363, 1193-1199, 10.1126/science.aau5153,
496 2019.

497 Haine, T. W. N., Curry, B., Gerdes, R., Hansen, E., Karcher, M., Lee, C., Rudels, B., Spreen,
498 G., Steur, L. d., Stewart, K. D., and Woodgate, R.: Arctic freshwater export: Status,
499 mechanisms, and prospects, *Global and Planetary Change*, 125, 13-35, 2015.

500 Håvik, L., Pickart, R. S., Våge, K., Torres, D., Thurnherr, A. M., Beszczynska-Möller, A.,
501 Walczowski, W., and Appen, W.-J. v.: Evolution of the East Greenland Current from Fram
502 Strait to Denmark Strait: Synoptic measurements from summer 2012, *J. Geophys. Res.*
503 *Oceans*, 122, 1974-1994, doi:10.1002/2016JC01222, 2017.

504 Khatiwala, S., Tanhua, T., Mikaloff Fletcher, S., Gerber, M., Doney, S. C., Graven, H. D.,
505 Gruber, N., McKinley, G. A., Murata, A., Ríos, A. F., and Sabine, C. L.: Global ocean storage
506 of anthropogenic carbon, *Biogeosciences*, 10, 2169-2191, 10.5194/bg-10-2169-2013, 2013.



- 507 Landschützer, P., Gruber, N., Bakker, D. C. E., Schuster, U., Nakaoka, S., Payne, M. R.,
508 Sasse, T. P., and Zeng, J.: A neural network-based estimate of the seasonal to inter-annual
509 variability of the Atlantic Ocean carbon sink, *Biogeosciences*, 10, 7793-7815, 10.5194/bg-10-
510 7793-2013, 2013.
- 511 Lebehoh, A. D., Halloran, P. R., Watson, A. J., McNeill, D., Ford, D. A., Landschützer, P.,
512 Lauvset, S. K., and Schuster, U.: Reconciling Observation and Model Trends in North
513 Atlantic Surface CO₂, *Global Biogeochemical Cycles*, 33, 1204–1222,
514 10.1029/2019gb006186, 2019.
- 515 Lee, K., Tong, L. T., Millero, F. J., Sabine, C. L., Dickson, A. G., Goyet, C., Park, G.-H.,
516 Wanninkhof, R., Feely, R. A., and Key, R. M.: Global relationships of total alkalinity with
517 salinity and temperature in surface waters of the world's oceans, *Geophysical Research*
518 *Letters*, 33, doi:10.1029/2006GL027207, 2006.
- 519 McClelland, J. W., Holmes, R. M., Dunton, K. H., and Macdonald, R. W.: The Arctic Ocean
520 Estuary, *Estuaries and Coasts*, 35, 353–368, DOI 10.1007/s12237-010-9357-3, 2012.
- 521 McKinley, G. A., Fay, A. R., Lovenduski, N. S., and Pilcher, D. J.: Natural Variability and
522 Anthropogenic Trends in the Ocean Carbon Sink, *Annu. Rev. Mar. Sci.*, 9, 125-150,
523 10.1146/annurev-marine-010816-060529, 2017.
- 524 Mikaloff Fletcher, S. E., Gruber, N., Jacobson, A. R., Doney, S. C., Dutkiewicz, S., Gerber,
525 M., Follows, M., Joos, F., Lindsay, K., Menemenlis, D., Mouchet, A., Iler, S. A. M.,
526 Sarmiento, J. L., et al. (2006), and *Global Biogeochem. Cycles*, GB2002,
527 doi:10.1029/2005GB002530.: Inverse estimates of anthropogenic CO₂ uptake, transport, and
528 storage by the ocean, *Global Biogeochem. Cycles*, 20, doi:10.1029/2005GB002530, 2006.
- 529 Nilsen, J. E. Ø., Hátún, H., Mork, K. A., and Valdimarsson, H.: The NISE Dataset. , Faroese
530 Fisheries Laboratory, Box 3051, Tórshavn, Faroe Islands, 2008.
- 531 Nondal, G., Bellerby, R., Olsen, A., Johannessen, T., and Olafsson, J.: Predicting the surface
532 ocean CO₂ system in the northern North Atlantic: Implications for the use of Voluntary
533 Observing Ships., *Limnology and Oceanography: Methods*, 7, 109-118, 2009.
- 534 Olafsson, J., Olafsdottir, S. R., Benoit-Cattin, A., and Takahashi, T.: The Irminger Sea and the
535 Iceland Sea time series measurements of sea water carbon and nutrient chemistry 1983–2008,
536 *Earth Syst. Sci. Data*, 2, 99-104, 10.5194/essd-2-99-2010, 2010.
- 537 Olsen, A., Omar, A. M., Bellerby, R. G. J., Johannessen, T., Ninnemann, U., Brown, K. R.,
538 Olsson, K. A., Olafsson, J., Nondal, G., Kivimae, C., Kringstad, S., Neill, C., and Olafsdottir,
539 S.: Magnitude and Origin of the Anthropogenic CO₂ Increase and ¹³C Suess Effect in the
540 Nordic Seas Since 1981, *Global Biogeochemical Cycles*, 20, GB3027,
541 doi:10.1029/2005GB002669, 2006.
- 542 Ouyang, Z., Qi, D., Chen, L., Takahashi, T., Zhong, W., DeGrandpre, M. D., Chen, B., Gao,
543 Z., Nishino, S., Murata, A., Sun, H., Robbins, L. L., Jin, M., and Cai, W.-J.: Sea-ice loss
544 amplifies summertime decadal CO₂ increase in the western Arctic Ocean, *Nature Climate*
545 *Change*, 10, 678-684, 10.1038/s41558-020-0784-2, 2020.
- 546 Ólafsson, J.: Connections between oceanic conditions off N-Iceland, Lake Mývatn
547 temperature, regional wind direction variability and the North Atlantic Oscillation, *Rit*
548 *Fiskideildar*, 16, 41-57, 1999.
- 549 Ólafsson, J.: Winter mixed layer nutrients in the Irminger and Iceland Seas, 1990-2000, *ICES*
550 *Marine Science Symposia*, 219, 329-332, 2003.
- 551 Qi, D., Chen, L., Chen, B., Gao, Z., Zhong, W., Feely, R. A., Anderson, L. G., Sun, H., Chen,
552 J., Chen, M., Zhan, L., Zhang, Y., and Cai, W.-J.: Increase in acidifying water in the western
553 Arctic Ocean, *Nature Clim. Change*, 7, 195-199, 10.1038/nclimate3228
554 [http://www.nature.com/nclimate/journal/v7/n3/abs/nclimate3228.html#supplementary-](http://www.nature.com/nclimate/journal/v7/n3/abs/nclimate3228.html#supplementary-information)
555 [information](http://www.nature.com/nclimate/journal/v7/n3/abs/nclimate3228.html#supplementary-information), 2017.



- 556 Rysgaard, S., Glud, R. N., Sejr, M. K., Bendtsen, J., and Christensen, P. B.: Inorganic carbon
557 transport during sea ice growth and decay: A carbon pump in polar seas, *Journal of*
558 *Geophysical Research*, 112, 2007.
- 559 Schlitzer, R.: Ocean Data View, <http://odv.awi.de>, 2018.
- 560 Schuster, U., McKinley, G. A., Bates, N., Chevallier, F., Doney, S. C., Fay, A. R., González-
561 Dávila, M., Gruber, N., Jones, S., Krijnen, J., Landschützer, P., Lefèvre, N., Manizza, M.,
562 Mathis, J., Metzl, N., Olsen, A., Rios, A. F., Rödenbeck, C., Santana-Casiano, J. M.,
563 Takahashi, T., Wanninkhof, R., and Watson, A. J.: An assessment of the Atlantic and Arctic
564 sea-air CO₂ fluxes, 1990–2009, *Biogeosciences*, 10, 607-627, 10.5194/bg-10-607-2013,
565 2013.
- 566 Serreze, M. C., and Meier, W. N.: The Arctic's sea ice cover: trends, variability, predictability,
567 and comparisons to the Antarctic, *Annals of the New York Academy of Sciences*, 1436, 36-
568 53, 10.1111/nyas.13856, 2019.
- 569 Stefánsson, U.: North Icelandic Waters, *Rit Fiskideildar*, 3, 1-269, 1962.
- 570 Sutherland, D. A., Pickart, R. S., Peter Jones, E., Azetsu-Scott, K., Jane Eert, A., and
571 Ólafsson, J.: Freshwater composition of the waters off southeast Greenland and their link to
572 the Arctic Ocean, *Journal of Geophysical Research: Oceans*, 114, 10.1029/2008jc004808,
573 2009.
- 574 Takahashi, T., J.Ólafsson, Broecker, W. S., J.Goddard, Chipman, D. W., and White, J.:
575 Seasonal variability of the carbon-nutrient chemistry in the ocean areas west and north of
576 Iceland, *Rit Fiskideildar*, 9, 20-36, 1985.
- 577 Takahashi, T., Ólafsson, J., Goddard, J. G., Chipman, D. W., and Sutherland, S. C.: Seasonal
578 variation of CO₂ and nutrient salts over the high latitude oceans: A comparative study,
579 *Global Biogeochem. Cycles*, 7, 843-878, 1993a.
- 580 Takahashi, T., Ólafsson, J., Goddard, J. G., Chipman, D. W., and Sutherland, S. C.: Seasonal
581 variation of CO₂ and nutrient salts over the high latitude oceans: A comparative study, *Global*
582 *Biogeochemical Cycles*, 7, 843-878, 1993b.
- 583 Takahashi, T., Sutherland, S. C., Sweeney, C., Poisson, A., Metzl, N., Tilbrook, T., Bates, N.,
584 Wanninkhof, R., Feely, R. A., Sabine, C., Olafsson, J., and Nojiri, Y.: Global sea-air CO₂ flux
585 based on climatological surface ocean pCO₂, and seasonal biological and temperature effects,
586 *Deep-Sea Research II*, 49, 1601-1622, 2002.
- 587 Takahashi, T., Sutherland, S. C., Wanninkhof, R., Sweeney, C., Feely, R. A., Chipman, D.
588 W., Hales, B., Friederich, G., Chavez, F., Sabine, C., Watson, A., Bakker, D. C. E., Schuster,
589 U., Metzl, N., Yoshikawa-Inoue, H., Ishii, M., Midorikawa, T., Nojiri, Y., Körtzinger, A.,
590 Steinhoff, T., Hoppema, M., Olafsson, J., Arnarson, T. S., Tilbrook, B., Johannessen, T.,
591 Olsen, A., Bellerby, R., Wong, C. S., Delille, B., Bates, N. R., and Baar, H. J. W. d.:
592 Climatological mean and decadal change in surface ocean pCO₂, and net sea-air CO₂ flux
593 over the global oceans, *Deep-Sea Research II*, 56, 554-577, doi:10.1016/j.dsr2.2008.12.009,
594 2009.
- 595 Takahashi, T., Sutherland, S. C., Chipman, D. W., Goddard, J. G., Ho, C., Newberger, T.,
596 Sweeney, C., and Munro, D. R.: Climatological distributions of pH, pCO₂, total CO₂,
597 alkalinity, and CaCO₃ saturation in the global surface ocean, and temporal changes at selected
598 locations, *Marine Chemistry*, 164, 95-125, <http://dx.doi.org/10.1016/j.marchem.2014.06.004>,
599 2014.
- 600 Tans, P., and Keeling, R.: Mauna Loa CO₂ monthly mean data. NOAA/ESRL (Ed.), 2019.
- 601 Våge, K., Pickart, R. S., Sarafanov, A., Knutsen, Ø., Mercier, H., Lherminier, P., van Aken,
602 H. M., Meincke, J., Quadfasel, D., and Bacon, S.: The Irminger Gyre: Circulation,
603 convection, and interannual variability, *Deep Sea Research Part I: Oceanographic Research*
604 *Papers*, 58, 590-614, <https://doi.org/10.1016/j.dsr.2011.03.001>, 2011.



605 Våge, K., Pickart, R. S., Spall, M. A., Moore, G. W. K., Valdimarsson, H., Torres, D. J.,
606 Y.Erofeeva, S., and Ø.Nilsen, J. E.: Revised circulation scheme north of the Denmark Strait,
607 Deep-Sea Research Part I, 79, 20–39, 2013.

608 Våge, K., Moore, G. W. K., Jónsson, S., and Valdimarsson, H.: Water mass transformation in
609 the Iceland Sea, Deep Sea Research Part I: Oceanographic Research Papers, 101, 98-109,
610 <http://dx.doi.org/10.1016/j.dsr.2015.04.001>, 2015.

611 Wanninkhof, R., Park, G. H., Takahashi, T., Sweeney, C., Feely, R., Nojiri, Y., Gruber, N.,
612 Doney, S. C., McKinley, G. A., Lenton, A., Le Quéré, C., Heinze, C., Schwinger, J., Graven,
613 H., and Khatiwala, S.: Global ocean carbon uptake: magnitude, variability and trends,
614 Biogeosciences, 10, 1983-2000, 10.5194/bg-10-1983-2013, 2013.

615 Wanninkhof, R.: Relationship between wind speed and gas exchange over the ocean revisited,
616 Limnol. Oceanogr.: Methods, 12, 351–362, DOI 10.4319/lom.2014.12.351, 2014.

617 Wanninkhof, R., and Triñanes, J.: The impact of changing wind speeds on gas transfer and its
618 effect on global air-sea CO₂ fluxes, Global Biogeochem. Cycles, 31,
619 doi:10.1002/2016GB005592, 2017.

620 Weiss, R. F.: Carbon dioxide in water and seawater: The solubility of a non-ideal gas, Marine
621 Chemistry, 2, 203-215, 1974.

622